

# Parameter-Optimized Design of a Longitudinal Viscous Damper for a Long-Span Railway Suspension Bridge

Yu Chen <sup>1</sup>, Ruoyu Han <sup>1,2,\*</sup> and Ren'an Yuan <sup>1,2</sup>

<sup>1</sup> China Railway Major Bridge Reconnaissance & Design Institute Co., Ltd., Wuhan 430056, Hubei Province, China;

<sup>2</sup> State Key Laboratory of Bridge Intelligent and Green Construction, Wuhan 430056, Hubei Province, China.

\* Correspondence: hanruoyu1992@qq.com

**Abstract:** To study the influence of viscous damper parameters on the mechanical behavior of long-span railway suspension bridges, a railway suspension bridge with a main span of 1,100 m and asymmetric towers was used as a case study. Using dynamic time-history analysis methods, different damping coefficients and velocity exponents were analyzed for their effects on the dynamic response of the bridge under both train crossing and E2 seismic conditions. The dynamic response results were compared, and a mechanism analysis of the damper's effect on the structural response was conducted. The computational results indicate that, for the train crossing condition, increasing the damping coefficient and decreasing the velocity exponent can reduce the longitudinal displacement at the beam ends while increasing the bending moment at the base of the towers; for the E2 seismic condition, increasing the damping coefficient can reduce the longitudinal displacement at the beam ends and decrease the bending moment at the base of the towers, whereas the value of the velocity exponent has little effect on the structure; the parameters of the dampers should consider various dynamic conditions to ensure control objectives while also considering the energy dissipation capacity and constructability. Finally, parameter design recommendations for nonlinear viscous dampers are proposed.

**Keywords:** railway suspension bridge; viscous damper; velocity exponent; damping coefficient

**Citation:** Chen, Y.; Han, R.; Yuan, R. Parameter-Optimized Design of a Longitudinal Viscous Damper for a Long-Span Railway Suspension Bridge. *Prestress Technology* 2024, 3, 11-19. <https://doi.org/10.59238/j.pt.2024.03.002>

Received: 16/07/2024

Accepted: 12/09/2024

Published: 30/09/2024

**Publisher's Note:** Prestress technology stays neutral with regard to jurisdictional claims in published maps and institutional affiliations.



**Copyright:** © 2024 by the authors. Submitted for possible open access publication under the terms and conditions of the Creative Commons Attribution (CC BY) license (<https://creativecommons.org/licenses/by/4.0/>).

## 1 Introduction

With the continuous advancement of technology, the span of railway bridges in China has surpassed the 1,000 m mark [1-4]. Unlike cable-stayed bridges, the asymmetric loading of trains on suspension bridges leads to significant longitudinal displacement at the ends of the bridge. Excessive longitudinal displacement at bridge ends can cause frequent and repetitive movements of track expansion adjustment devices, deteriorate the bearings and suspender cables, and adversely affect the normal operation of railway suspension bridges [5-8].

Longitudinal viscous dampers are often installed at the tower-beam connections of railway suspension bridges to limit the longitudinal displacement at the ends [4,9]. Determining the appropriate parameters for these dampers is crucial to designing large-span railway suspension bridges.

The damping force of a viscous damper can be calculated via the following formula(1) [10]:

$$F_d = CV^\alpha \quad (1)$$

where  $C$  is the damping coefficient (in units of  $kN \cdot (m/s)^{-\alpha}$ , with subsequent units omitted),  $V$  is the relative velocity between the two ends of the damper (in units of m/s), and  $\alpha$  is the velocity index, which is dimensionless. When  $\alpha = 1$ , the damper is a linear viscous damper, and when  $\alpha < 1$ , it is a nonlinear viscous damper. In recent years, viscous dampers with a velocity index  $\alpha$  as low as 0.1 have been developed in China [11]. According to the standards for viscous dampers used in

bridges [12], the maximum damping force of a single viscous damper is 4,000 kN, and the velocity indices available are 0.1, 0.2, 0.3, 0.4, 0.5, 0.6, and 1.0.

The selection of an appropriate damper requires the determination of the appropriate values for the damping coefficient ( $C$ ) and the velocity index ( $\alpha$ ). Existing research has focused primarily on highway suspension bridges. For example, Song et al. [13] analyzed the impact of damper parameters on the end displacement of the Xiangxi Bridge, whereas Long et al. [14] studied the effects of damper parameters on the seismic response of the Kaizhou Lake Grand Bridge. However, research on the selection of damper parameters for railway suspension bridges is scarce. Owing to the characteristics of train loads—such as heavy loads, constant speed, and concentrated distribution—and the precision required in the construction of track expansion adjustment devices at bridge ends, railway suspension bridges are more sensitive to longitudinal displacement at the ends of the bridge. Therefore, the control requirements for railway suspension bridges are much higher than those for highway bridges. Given this research gap, this paper analyzes train crossing and seismic response under different damper parameters for a high–low tower railway suspension bridge to explore reasonable methods for selecting damper parameters for railway suspension bridges.

## 2 Project Background

A double-track railway steel truss suspension bridge with a high–low tower suspension bridge and a main span of 1,100 m was used for analysis in this study. The span arrangement is 140 m + 1100 m + 100 m (see Figure 1). The main towers are constructed of reinforced concrete; the height of the left high tower is approximately 260 m, and the height of the right low tower is approximately 145 m. The tops of both towers are at the same elevation, with a distance of 127 m from the top of the towers to the bridge deck. The structure features a floating system in the longitudinal direction, with 8 flexible central clamps set between the main cables and the stiffening beam at the midpoint of the span. Each tower's connection to the beam is equipped with 8 longitudinal viscous dampers.

Finite element software was used to perform nonlinear static calculations of the bridge in its completed state. After a reasonably complete bridge state with a "tower-straight-beam" was obtained, the stress stiffness under dead loads was incorporated for dynamic time-history analysis under train crossing and E2 earthquake conditions. The train live load is specified as the ZKH load (Train Load Diagrams of Mixed Passenger and Freight Railway) [15], with a loading length of 550 m and a design speed of 120 km/h. The analysis considers only the condition of a single train crossing the bridge.

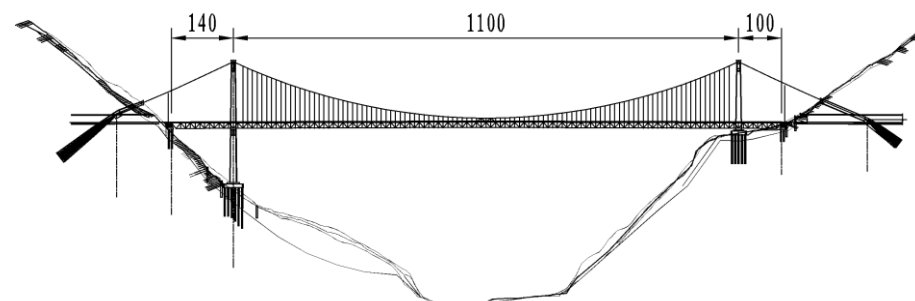


**Figure 1** Elevation of the suspension bridge (Unit: m)

## 3 Impact of Various Damper Parameters on the Effects of Train Crossing

A finite element model of the aforementioned bridge was established via spatial finite element software. In this model, the main cables and hangers were simulated via cable elements, the main towers and steel truss girders were modeled via beam

elements, and the bridge deck plate was represented by plate elements. The entire bridge consists of 4,470 nodes and 12,163 elements. Initially, the stress-free lengths of each segment of the main cables and the hangers were determined through the shape-finding method for the suspension bridge. A static analysis of the completed bridge state was subsequently performed, considering geometric nonlinearity, to achieve a target state of the “vertical tower and horizontal beam”. On this basis, the stress stiffness of each element under constant loads was included, and a dynamic time-history analysis of the train crossing the bridge was carried out.

The live load of the train is defined as the ZKH load according to the "Train Load Diagrams" [15], with a loading length of 550 m and a design speed of 120 km/h. Only the single-track train crossing scenario was considered for dynamic time-history analysis. The Newmark constant acceleration direct integration method was used for nonlinear dynamic time-history analysis. The nonlinear viscous damper was modeled via the Maxwell model (Figure 2), with the stiffness of the series spring set at  $1,000C$  (kN/m). The damping coefficient ( $C$ ) values used were 1,000, 1,500, 2,000, 2,500, and 3,000, while the velocity index ( $\alpha$ ) values used were 0.1, 0.2, 0.3, 0.5, and 1.0. The end displacement of the beams and the bending moment at the base of the towers were calculated for different damper parameters.



Figure 2 Maxwell viscous damper model

First, we considered the impact of different values of the velocity index  $\alpha$  on the effect of train crossing. When the damping coefficient  $C$  is set to 1,500 and 2,500, the longitudinal displacement at the structure beam ends was calculated for velocity indices  $\alpha$  of 0.1, 0.2, 0.3, 0.5, and 1.0, as well as for the case without dampers. Since the trends on the high-tower side and the low-tower side are nearly consistent, only the longitudinal displacement at the beam ends on the high-tower side is illustrated in Figure 3.

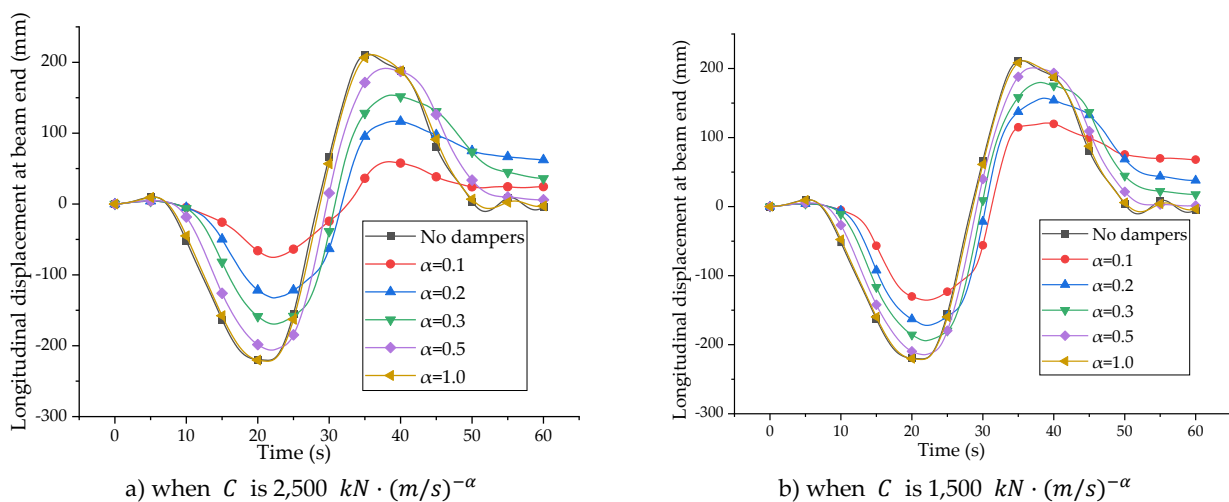


Figure 3 Time history curves of the longitudinal displacement at the beam end for different  $\alpha$  values under train crossing conditions

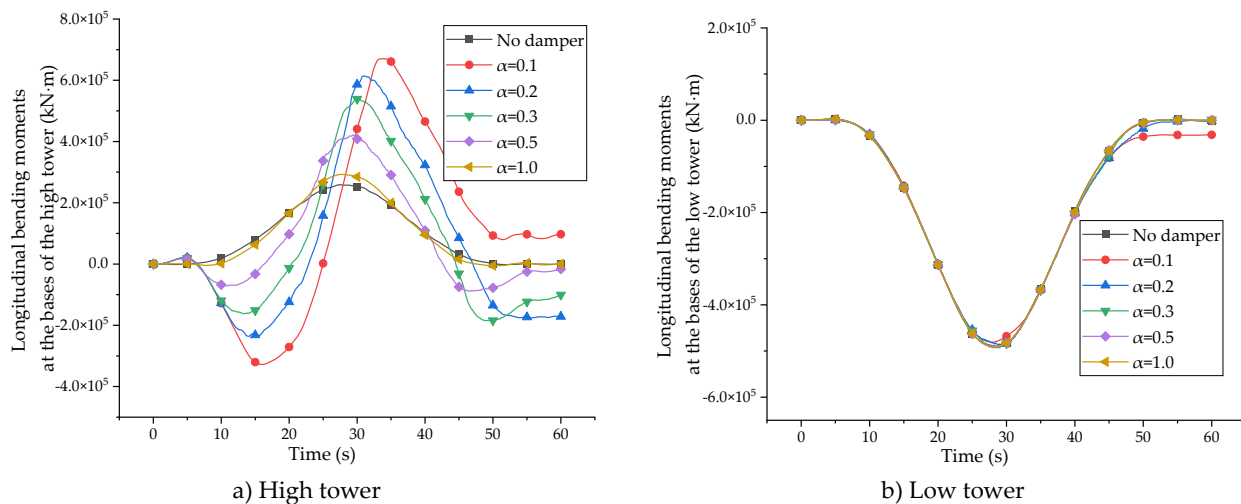
From Figure 3, the following can be observed:

- (1) When the train travels across the left and right spans, the longitudinal displacement curve at the beam ends exhibits distinct troughs and peaks.
- (2) As the velocity index  $\alpha$  decreases, the amplitude of the longitudinal displacement at the beam ends tends to decrease.

- (3) When  $C$  is 2,500, adjusting the velocity index  $\alpha$  has a more noticeable effect, whereas when  $C$  is 1,500, the influence of  $\alpha$  is less significant.
- (4) When  $\alpha$  is 1.0, there is not much difference in the displacement amplitude compared to the case without dampers.

According to Equation (1), under different velocity indices, the damping force ( $F_d$ ) exhibits different nonlinear trends: When the movement speed of the beam body is low, lower index ( $\alpha$ ) values are associated with greater damping forces. Under the condition of train crossing, the movement speed of the main beam is relatively low, approximately 0.05 m/s, so lower  $\alpha$  values are associated with stronger damping effect, resulting in smaller longitudinal displacement amplitudes at the beam ends. When the movement speed of the main beam increases, the differences caused by different  $\alpha$  values gradually diminish. At a speed of 1.0 m/s, regardless of the value of  $\alpha$ , the results are completely consistent. Therefore, when the damping coefficient  $C$  is small, an increase in speed leads to a reduced sensitivity of the beam end displacement to changes in  $\alpha$ .

Next, we examine the impact of different velocity indices  $\alpha$  on the longitudinal bending moment at the bases of the high tower and the low tower when  $C$  is 2,500, as shown in Figure 4.



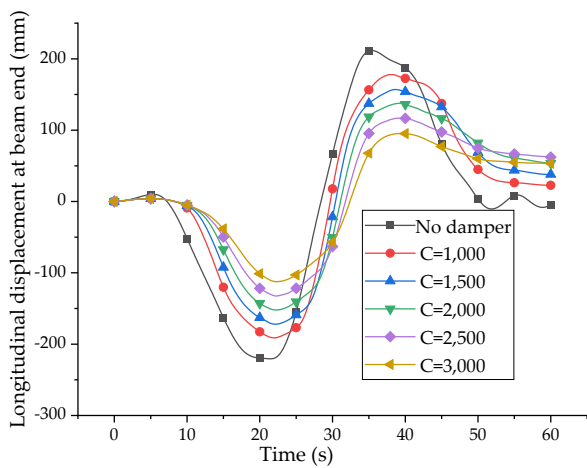
**Figure 4** Time history curves of the bending moment at the tower bottom for different  $\alpha$  values under train crossing conditions

Figure 4 clearly shows that the effect of the velocity index on the bending moments at the bases of the two towers has distinct patterns. For the high tower, as the velocity index  $\alpha$  decreases, the bending moment amplitude increases gradually, and the curve shape transitions from a single peak to a sinusoidal pattern. In contrast, the bending moment at the base of the low tower shows little change in trend or amplitude.

The longitudinal bending moment at the base of the tower consists of two parts: the unbalanced horizontal force at the top of the tower caused by the train load transmitted through the main cable and the horizontal force transferred from the damper to the lower transverse beam of the main tower. When there is no damper, the unbalanced horizontal force at the top of the tower due to the vertical load of the train reaches its maximum when the train travels to the midspan, causing the bending moment time-history curve to exhibit a single peak (or trough) shape. In the case with dampers, the distance between the damper and the tower base is approximately 130 meters for the high, whereas the distance is only approximately 5 meters for the low tower. Therefore, the damping force significantly affects the bending moment at the

base of the high tower but has almost no effect on the bending moment at the base of the low tower. With the reduction in the velocity index ( $\alpha$ ), the bending moment at the high tower generated by the damping force gradually becomes dominant, eventually resembling a sine wave curve. Therefore, in addition to examining the longitudinal displacement at the beam ends, the impact of  $\alpha$  on the bending moment at the base of the tower must also be considered, ensuring that the displacement control of the main beam meets the resistance requirements at the base of the main tower.

To analyze the impact of the damping coefficient ( $C$ ) on the structural response, according to the earlier figures, when the velocity index ( $\alpha$ ) is greater than 0.5, the damping force is small, and the damper effect is not significant, with little difference between the curves and the case without dampers. Therefore, when the velocity index ( $\alpha$ ) is 0.2, the structural responses for  $C$  values of 1,000, 1,500, 2,000, 2,500, and 3,000 are compared. Figure 6 shows the time history curve of the longitudinal displacement at the beam end on the high-tower side. Figure 6 shows the time history curve of the bending moment at the base of the high tower.



**Figure 5** Time history curve of longitudinal displacement at beam end on the high-tower side of different  $C$  under train crossing condition

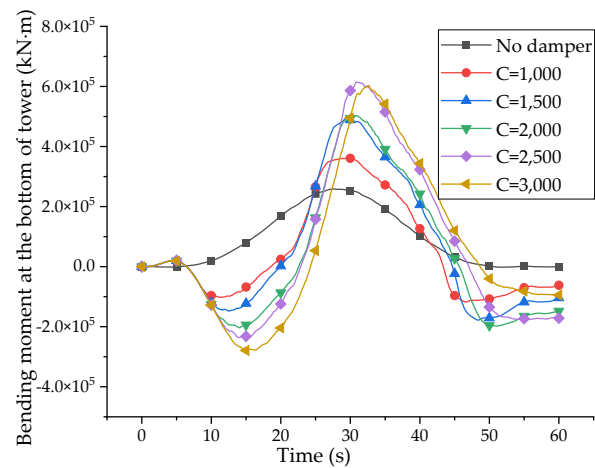


**Figure 6** Time history curve of bending moment at the base of high-tower of different  $C$  under train crossing condition

Figures 5 and 6 show that since the damping coefficient ( $C$ ) is directly proportional to the damping force, as  $C$  increases, the amplitude of the structural longitudinal displacement decreases, whereas the amplitude of the bending moment at the base of the high tower increases. Additionally, the shape of the time-history curve of the bending moment transitions from a single peak to a sinusoidal pattern.

#### 4 Effects of Various Damper Parameters on Seismic Effects

Typically, in small earthquakes, the structure operates at low speeds, and the dampers should meet normal usage requirements. In large earthquakes, dampers should effectively reduce displacement and mitigate structural damage while allowing for damper destruction and replacement. The working range and parameter selection of the damper in small earthquakes are similar to those when a train crosses the bridge. The focus here is on large earthquake scenarios.

This bridge is located in a high-seismic-intensity area, and the E2 seismic wave used in the calculations has a peak acceleration of approximately  $6 \text{ m/s}^2$ . A consistent excitation is applied for the dynamic time-history analysis. Considering a damping coefficient  $C = 2,500$ , the effects of different velocity indices ( $\alpha$ ) on the longitudinal displacement at the beam end and the bending moment at the base of the high tower are calculated, as shown in Figures 7 and 8.

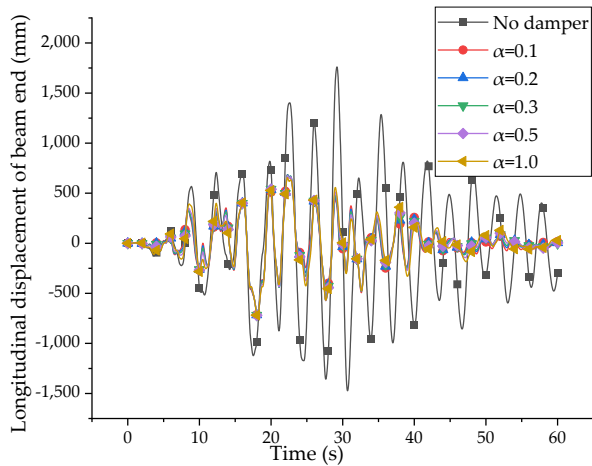


**Figure 7** Time history curve of longitudinal displacement at beam end of different  $\alpha$  under E2 earthquake condition

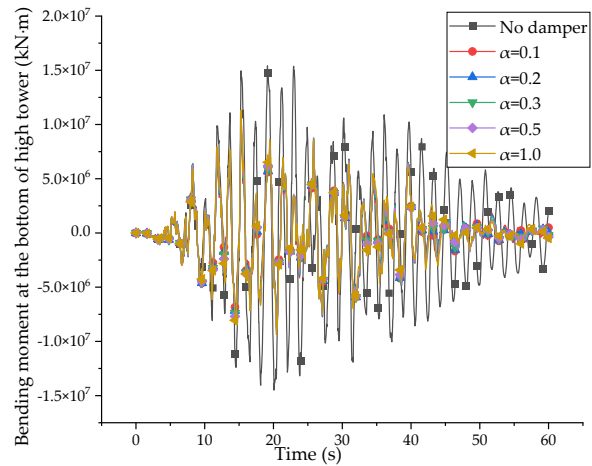


**Figure 8** Time history curve of bending moment at high-tower bottom of different  $\alpha$  under E2 earthquake condition

Figures 7 and 8 show that the installation of dampers can effectively reduce the longitudinal displacement at the beam ends and the bending moment at the base of the tower caused by earthquakes. However, under different velocity indices ( $\alpha$ ), the time–history curves largely overlap, with very little difference in trend and amplitude, which is notably different from the conditions during train crossing.

To understand this response, the damper velocity time–history curves for  $\alpha = 1.0$  and  $\alpha = 0.2$  shown in Figure 9. In the figure, the peak motion velocity of both dampers is 1.7 m/s, with a significant portion of the velocity range fluctuating at approximately 1.0 m/s. The previous analysis revealed that the velocity index ( $\alpha$ ) is sensitive to low-speed movements but insensitive to high-speed movements. When the velocity is 1.0 m/s, the value of  $\alpha$  does not affect the outcome. Therefore, when the velocity is near zero, the two curves show some differences, but when the velocity is higher, the curves basically coincide, and the amplitudes of the structural response are not significantly different.

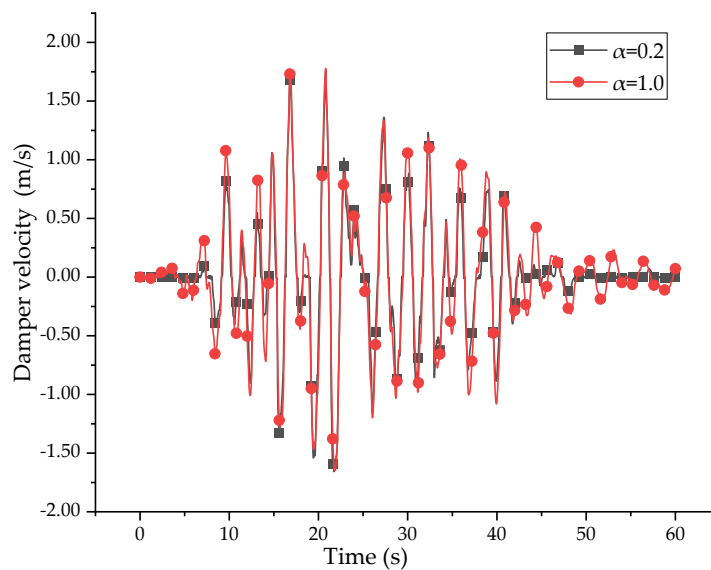


**Figure 9** Time history curve of the damper velocity under E2 earthquake conditions

Next, with a velocity index  $\alpha = 0.2$ , we examine the effects of different damping coefficients ( $C$ ) on the longitudinal displacement at the beam end and the bending

moment at the base of the high tower. The trends of the time–history curves are similar to those described previously and are not plotted again. Only the trends in the variation in response amplitude are presented, as shown in Figure 10.

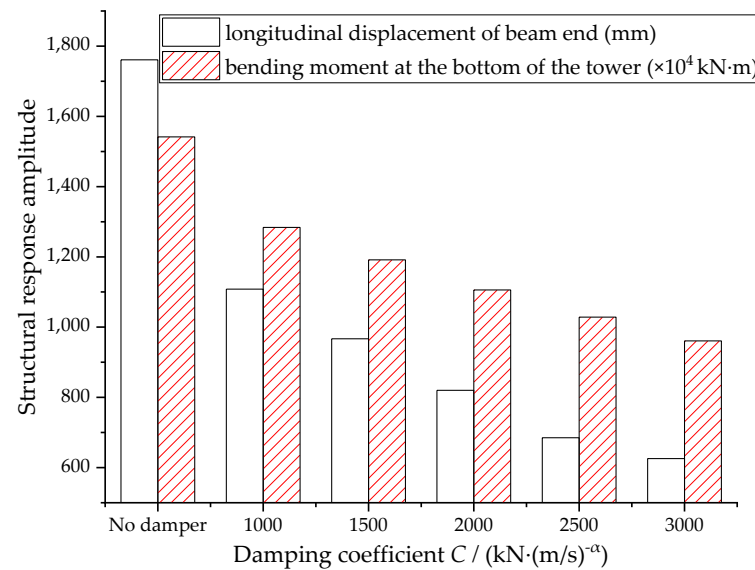


**Figure 10** Structure response amplitudes of different  $C$  values under E2 earthquake conditions

Figure 10 shows that as the damping coefficient ( $C$ ) increases, the longitudinal displacement at the beam end and the bending moment at the base of the tower under the E2 earthquake continuously decrease. However, the rate of reduction gradually slows; this indicates that increasing the damping coefficient ( $C$ ) can effectively limit structural displacement and reduce the base bending moment, but the effect becomes less significant beyond a certain point.

## 5 The Principles for Selecting the Damping Parameters

Based on the above analysis, to achieve good overall benefits for the damper under different conditions, the principles for selecting its parameters are summarized as follows:

### (1) Velocity index

Under the E2 earthquake, the impact of different velocity indices ( $\alpha$ ) on the structural response is minimal, so the  $\alpha$  value is primarily determined by the characteristics of the train crossing the bridge. For train crossing conditions, a smaller  $\alpha$  result in a smaller longitudinal displacement at the beam end but simultaneously increases the damping force, which may lead to higher base bending moments and highlight fatigue issues in the damper connection components. Therefore, to ensure good displacement control by the damper, a lower  $\alpha$  value, which generally does not exceed 0.5, is recommended.

### (2) Damping coefficient

Under the E2 earthquake, with high structural motion speeds, the impact of the velocity index  $\alpha$  is not significant. Instead, the structural displacement and bending moment at the base of the tower should be controlled by adjusting the damping coefficient. However, as the damping coefficient ( $C$ ) increases beyond a certain point, its effectiveness gradually diminishes, and a higher  $C$  also increases the bending moment at the base of the tower. Thus,  $C$  should not be excessively large. Additionally, an excessively high  $C$  may lead to excessive damper stiffness, reducing energy dissipation by limiting reciprocal displacement. Therefore, the selection of  $C$  should consider not only displacement control and internal forces but also energy dissipation effectiveness, economic factors, and construction space.

From the perspective of the load occurrence probability for long-span railway suspension bridges, train crossing conditions continuously occur, whereas the probability of E2 earthquake conditions is extremely low. Therefore, dampers should primarily meet the requirements for train crossing conditions, mainly to reduce longitudinal displacements at the beam ends to ensure the long-term performance of track expansion joints. In this context, the performance of dampers is primarily related to their stiffness for train crossings, whereas for E2 earthquakes, the focus is on their energy dissipation performance.

## 6 Conclusions

This paper presents a comparative analysis of damper parameters for a high-low-tower railway suspension bridge, leading to the following conclusions.

- (1) Under train crossing conditions, as the damper's velocity index  $\alpha$  decreases, the longitudinal displacement at the ends of the suspension bridge's beam decreases. Consequently, the bending moment at the base of the high tower increases gradually, whereas the bending moment at the base of the low tower remains unchanged. As the damping coefficient  $C$  increases, the longitudinal displacement at the beam ends decreases, and the bending moment at the base of the high tower increases.
- (2) Under E2 earthquake conditions, as the damping coefficient  $C$  of the damper increases, both the longitudinal displacement at the end of the suspension bridge beam and the bending moment at the base of the high tower decrease. However, the reduction becomes less pronounced with increasing  $C$ . Additionally, owing to the high velocity of beam movement, the velocity index  $\alpha$  has a minimal impact on the structural response.
- (3) When selecting damper parameters, various dynamic conditions, such as train crossings, small earthquakes, and large earthquakes, should be considered comprehensively. The damping coefficient ( $C$ ) is mainly determined by factors such as displacement, internal force control targets, and energy dissipation capability under large earthquakes and should not be excessively large. The velocity index ( $\alpha$ ) is primarily determined by the control target for longitudinal displacement at the beam end but should also consider the base bending moment and fatigue issues in the damper connections, and the value of the velocity index ( $\alpha$ ) should not be too small.

**Conflict of Interest:** All authors disclosed no relevant relationships.

**Data Availability Statement:** The data that support the findings of this study are available from the corresponding author, Han, upon reasonable request.




## References

1. Qin, S.; Xu, W.; Lu, Q.; Zheng, Q.; Fu, Z.; Yuan, R.; Sun, J. Overall Design and Concept Development for Main Navigational Channel Bridge of Changtai Changjiang River Bridge. *Bridge Construction* **2020**, *50*, 1-10, doi:10.3969/j.issn.1003-4722.2020.03.001.
2. Gao, Z.; Mei, X.; Xu, W.; Zhang, Y. Overall Design of Hutong Changjiang River Bridge. *Bridge Construction* **2015**, *45*, 1-6.
3. Chen, L.; Zhou, Y. Development and Practice of High-speed Railway Bridge Technology in China. *High Speed Railway Technology* **2020**, *11*, 27-32, doi:10.12098/j.issn.1674-8247.2020.02.005.
4. Tang, H.; Xu, G.; Liu, H. Overall Design of Main Bridge of Wufengshan Changjiang River Bridge. *Bridge Construction* **2020**, *50*, 1-7, doi:10.3969/j.issn.1003-4722.2020.06.001.
5. Wan, T.; Li, S. Longitudinal Displacement Characteristics and Longitudinal Supporting Requirements for Long-Span Railway Suspension Bridge. *Bridge Construction* **2020**, *50*, 29-35, doi:10.3969/j.issn.1003-4722.2020.04.005.



6. Guo, H.; Su, P.; Zhao, X.; Liu, X.; Le, S. Displacement Characteristics at Girder End of Long Span Railway Suspension Bridge Under Design Loads. *Railway Engineering* **2019**, *59*, 14-19, doi:10.3969/j.issn.1003-1995.2019.01.04.
7. Huang, G.; Hu, J.; Wan, T.; Hua, X.; Feng, Z.; Chen, Z. Characteristics and Mechanism of Longitudinal Displacement for Suspension Bridge under Vertical Loads. *Journal of Hunan University (Natural Sciences)* **2023**, *50*, 78-89, doi:10.16339/j.cnki.hdxzbzkb.2023.01.008.
8. Huang, G.; Hu, J.; Hua, X.; Wang, L.; Cui, J. Girder end longitudinal displacement mechanism of long-span suspension bridge under moving vehicles. *Journal of Vibration and Shock* **2021**, *40*, 107-115, doi:10.13465/j.cnki.jvs.2021.19.014.
9. Xu, W.; Li, S.; Hu, W. Design of Truss Stiffening Girder of a Long-Span Railway Suspension Bridge. *Bridge Construction* **2021**, *51*, 10-17, doi:10.3969/j.issn.1003-4722.2021.02.002.
10. Wang, Z.; Chai, X.; Ma, C. Research of Dampers Used to Mitigate Vibrations for Bridge Structures and Their Application. *Bridge Construction* **2019**, *49*, 7-12.
11. Wan, T. Performance Requirements of Viscous Dampers for Improvement of Durability of Bridge Structures. *Bridge Construction* **2016**, *46*, 29-34.
12. Ministry of transport of the people's Republic of China JT/T 926—2014 Fluid Vicious Damper for Bridges. 2014.
13. Song, X.; Huang, G.; Sun, Z.; Wang, L. Assessment and Design of Mitigation of Longitude Displacement of Suspension Bridges. *Highway Engineering* **2021**, *46*, 104-109, doi:10.19782/j.cnki.1674-0610.2021.04.015.
14. Long, P.; Du, B.; Tang, Z.; Zhang, J. Research on Optimization of Damper System for Long-span Suspension Bridge with Steel Truss Girder in Mountainous Area. *Transportation Science & Technology* **2022**, 51-55, doi:10.3963/j.issn.1671-7570.2022.03.011.
15. National Railway Administrallon of the People's Repulic of China TB/T 3466—2016 Code for Train Loads Diagrams. 2016.

AUTHOR BIOGRAPHIES

	<p><b>Yu Chen</b> M.E. Senior Engineer. China Railway Major Bridge Reconnaissance &amp; Design Institute Co., Ltd. Research Direction: Modern Bridge and Bridge Structure Design Theory. Email: 13871573232@qq.com</p>		<p><b>Ruoyu Han</b> M.E. Engineer. China Railway Major Bridge Reconnaissance &amp; Design Institute Co., Ltd. Research Direction: Bridge Design and Research. Email: hanruoyu1992@qq.com</p>
	<p><b>Ren'an Yuan</b> Ph.D. Senior Engineer. China Railway Major Bridge Reconnaissance &amp; Design Institute Co., Ltd. Research Direction: Construction Control Theory of Long-span Bridges. Email: 627948171@qq.com</p>		